

# DYNAMIC SIMULATION OF PROCESSING HIGH-ARSENIC COPPER CONCENTRATES IN A FLUIDIZED BED ROASTER

Ashish Rajoria, Luis Lucena, ANDRITZ Chile Ltda., Santiago, Chile  
 Suvajit Das, Marian Szatkowski, ANDRITZ Inc., Decatur, GA, United States  
 Igor Wilkomirsky, University of Concepcion, Concepcion, Chile

Presented at SME Annual Meeting/Exhibit, February 24-26, 2014, Salt Lake City, UT, USA

## Abstract

A dynamic process model for predicting the fluidized bed roasting of copper concentrates with high arsenic content is presented in this work. Mass and energy balances were performed based on roasting mechanism derived from thermodynamic data of species. The reaction rate data, obtained from pilot plant studies on major reactions, were used in tuning the kinetic parameters of the model.

IDEAS, a dynamic simulation package, is used in setting up the fluidized bed roaster plant model. The effect of process parameters such as concentrate feed rate, concentrate composition, airflow and cooling water rate on the temperature and conversion of roasting reactions are analyzed. The plant model captures the highly transient conditions occurring during the plant start-up, shutdown and other process perturbations. The application of this model in constructing a virtual plant environment for validating the operating procedures and operator training is presented.

**Keywords:** Fluidized Bed Roaster, Roasting Mechanism, Kinetic Parameters, Virtual Plant, Operator Training.

## Introduction

Roasting is a suitable pretreatment for the removal of high levels of impurities such as arsenic (As), antimony (Sb) and bismuth (Bi) from copper concentrate prior to smelting under oxidized condition. The process includes a fluidized bed roaster where most of the sulfide is oxidized to SO<sub>2</sub>, and the arsenic, along with the other impurities, is volatilized into the gas stream. The partially desulfurized calcine from the roaster is cooled and fed to the smelter to recover the metal.

The off-gas from the roaster containing SO<sub>2</sub>, dust and volatilized impurities - including arsenic compounds - is dedusted in cyclones, adiabatically cooled and further dedusted in a hot gas electrostatic precipitator. The resultant

gas passes to the wet gas cleaning section, where it is humidified and wet-scrubbed in a radial flow venturi. The bulk of the arsenic is removed to the scrubbing liquor which is sent to effluent treatment. The gas from the venturi is then cooled, and residual impurities in the gas are removed in wet electrostatic precipitators. The gas then passes to a double absorption contact acid plant where it is dried. The SO<sub>2</sub> is converted to SO<sub>3</sub> in the converter, and the SO<sub>3</sub> is absorbed in acid to produce sulfuric acid (H<sub>2</sub>SO<sub>4</sub>).

The dust from the roaster hot gas cleaning is cooled and stored for further processing.

In this article, a dynamic process model is presented for predicting the fluidized bed roasting of copper concentrates with high arsenic content using a simulation package called IDEAS [22].

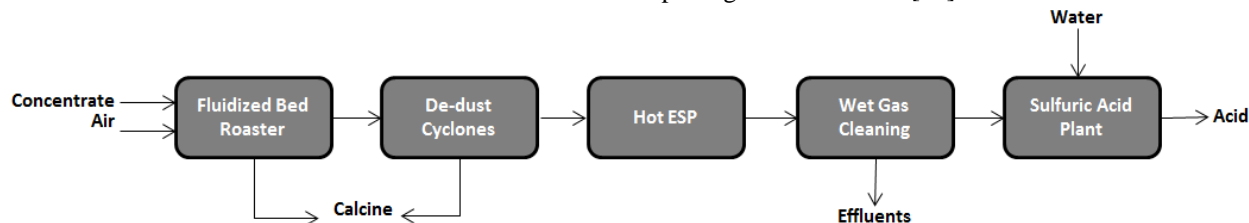
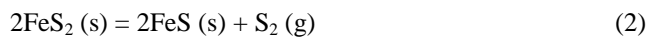


Figure 1. Block diagram of copper concentrate roasting plant.

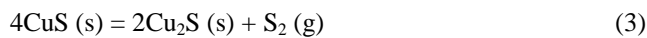
This process model is then used to validate a cold start-up procedure as well as to study the effect of change in concentrate feed flow rate, fluidizing airflow rate, cooling water rate, and concentrate feed composition on the temperature profile of the fluidizing bed, and also on the arsenic volatilization.

### Roasting Mechanism

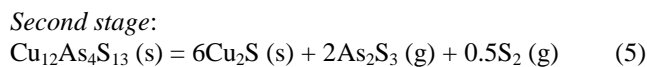
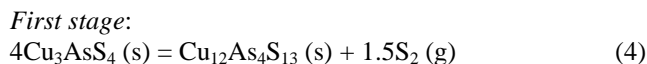
The concentrate feed entering the roaster typically consists of components such as enargite ( $\text{Cu}_3\text{AsS}_4$ ), pyrite ( $\text{FeS}_2$ ), and covelite ( $\text{CuS}$ ). The decomposition of both enargite and the associated pyrite is outlined in the following reactions [9, 17, 18, 20]:



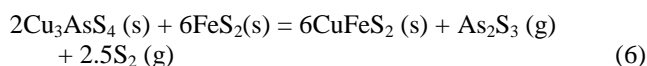
Also, the decomposition of the associated copper (II) sulfide ( $\text{CuS}$ ) to form copper (I) sulfide is as outlined below:



It was concluded that enargite decomposition proceeded in two consecutive stages through tennantite ( $\text{Cu}_{12}\text{As}_4\text{S}_{13}$ ) formation as an intermediate compound and subsequently to chalcocite ( $\text{Cu}_2\text{S}$ ) according to [12, 13]:



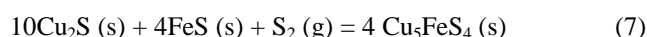
It was also predicted that at low partial pressures, in the presence of pyrite, enargite converts to chalcocopyrite ( $\text{CuFeS}_2$ ) and chalcocopyrite-like compounds according to the following reaction [18]:



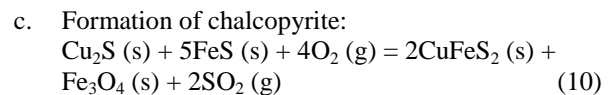
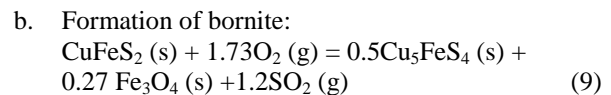
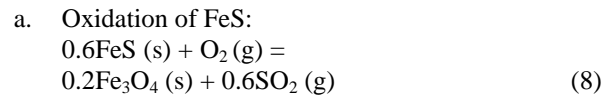
The by-product formed in the above reactions (1 to 6) will in turn react further to produce additional products [6, 10, 15].

It is also probable that, in the presence of oxygen, the species undergo oxidation reactions instead of decomposition reactions.

Also, bornite can be formed according to the following reaction [19]:

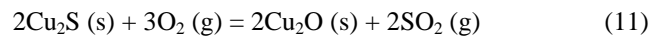


An undesired by-product of roasting is the formation of magnetite ( $\text{Fe}_3\text{O}_4$ ). Magnetite reacts with the arsenic present in the concentrate and forms stable iron-arsenate which ends up in the roasted material there by reducing the overall arsenic removal efficiency [11, 12]. It is virtually impossible to control the magnetite formation, which can be formed in three ways:

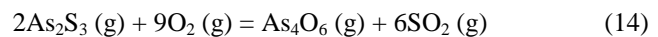
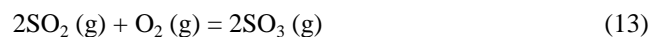


In order to limit the amount of magnetite produced during roasting, airflow rate or oxygen potential to magnetite should be controlled.

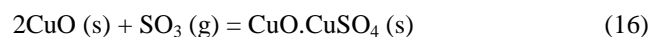
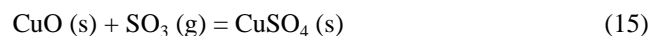
During the conversion of copper sulfide to oxide, chalcocite ( $\text{Cu}_2\text{S}$ ) converts to copper (I) oxide ( $\text{Cu}_2\text{O}$ ) before forming copper (II) oxide ( $\text{CuO}$ ).



In the presence of oxygen, the gases oxidize based on the following equations [11, 18]:



The production of sulfur trioxide ( $\text{SO}_3$ ) gas as outlined in reaction 13 is critical in the formation of sulfates. The sulfation of copper oxides by sulfur trioxide has been described according to the following reactions [6]:

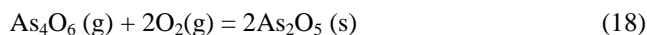


The sulfation reaction can proceed directly as outlined in reaction 15 based on the prior oxidation of the sulfides as given in reaction 6 and the formation of the sulfating sulfur trioxide ( $\text{SO}_3$ ) gas in reaction 13. Alternatively, the formation of an intermediate oxy-sulfate, as presented in reaction 16, followed by sulfation of the oxy-sulfate as

shown in reaction 17 can occur. As the roasting temperature increases beyond 700°C, these reactions begin to reverse and the sulfates decompose.

It was found that when the concentrate is partially roasted at temperatures above approximately 725°C, some stickiness followed by agglomeration or sintering of the calcine may occur [12].

It was suggested that arsenic trioxide gas (As<sub>4</sub>O<sub>6</sub>) will oxidize to arsenic pentoxide (As<sub>2</sub>O<sub>5</sub>) in the calcine, under highly sulfating conditions between 500 and 650°C, according to the reaction [4, 7]:



It was also found that arsenic was removed as arsenic trioxide in the gas stream due to its high vapor pressure [2]. As the roasting temperature increases, rate of arsenic removal also increases.

As described in this section, there are several reactions that can happen during the roasting process. In order to model this process it is essential to understand the kinetic and thermodynamic constraints so that the end product can be accurately predicted as a function of temperature, pressure, and limiting reactants.

## Thermodynamic Analysis

Assuming that the roasting reactions follow first order kinetics [3], reaction rate can be described as the product of kinetic constant  $k$ , which depends on temperature, and a reactant concentration function, which is temperature-independent, in the form:

$$\frac{dX}{dt} = -kf(X) \quad (19)$$

The dependency of the kinetic constant on the temperature can be expressed by the Arrhenius relationship:

$$k = Ae^{-\frac{E_a}{RT}} \quad (20)$$

where

- $A$  is a constant;
- $E_a$ , the activation energy;
- $R$ , the gas constant;
- $T$ , the absolute temperature.

Data from the plant pilot study carried out by Wilkomirsky at the University of Concepcion (Unpublished work) was used to calculate residence time and extent of reaction. This information was then used to derive kinetic parameters for use in the process model.

A thermochemical programming tool called ChemApp was integrated with IDEAS simulation package to formulate multicomponent reaction mechanism and determination of associated energy balances [21]. Heat of reaction for major reactions taking place in the roaster is shown in Table 1.

**Table 1.** Heat of reaction for major reactions taking place in the roaster.

Reactions	Heat of Reaction ( $\Delta H_{\text{rxn}}^0$ ), kJ/kg
$2\text{Cu}_3\text{AsS}_4 (\text{s}) = 3\text{Cu}_2\text{S} (\text{s}) + \text{As}_2\text{S}_3 (\text{g}) + \text{S}_2 (\text{g})$	(-)132.42*
$2\text{FeS}_2 (\text{s}) = 2\text{FeS} (\text{s}) + \text{S}_2 (\text{g})$	1,118.32
$4\text{CuS} (\text{s}) = 2\text{Cu}_2\text{S} (\text{s}) + \text{S}_2 (\text{g})$	455.96
$10\text{Cu}_2\text{S} (\text{s}) + 4\text{FeS} (\text{s}) + \text{S}_2 (\text{g}) = 4\text{Cu}_3\text{FeS}_4 (\text{s})$	(-)257.75*
$0.6\text{FeS} (\text{s}) + \text{O}_2 (\text{g}) = 0.2\text{Fe}_3\text{O}_4 (\text{s}) + 0.6\text{SO}_2 (\text{g})$	(-)6,457.35*
$\text{S}_2 (\text{g}) + 2\text{O}_2 (\text{g}) = 2\text{SO}_2 (\text{g})$	(-)11,255.48*
$2\text{As}_2\text{S}_3 (\text{g}) + 9\text{O}_2 (\text{g}) = \text{As}_4\text{O}_6 (\text{g}) + 6\text{SO}_2 (\text{g})$	(-)6,160.16*

Source: ChemApp [21]

\*(-) indicates the reaction is exothermic.

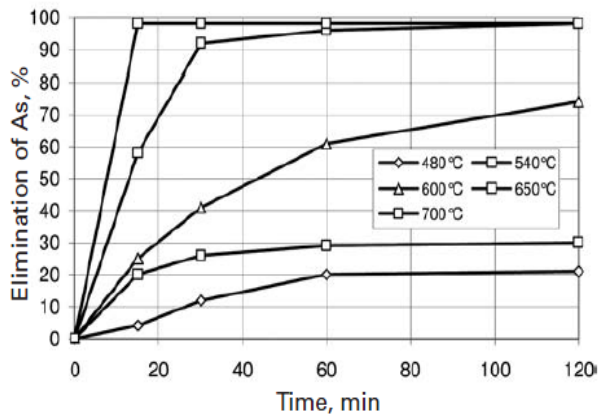


**Figure 2.** Arsenic removal as a function of time and temperatures during enargite-bearing copper concentrate roasting in a fixed bed [5].

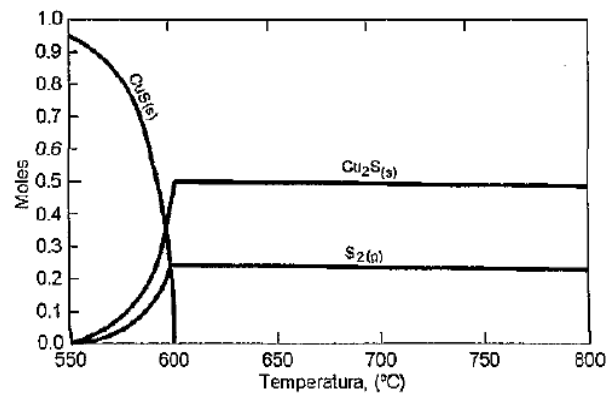


**Figure 4.** Equilibrium phases for the decomposition of covelite ( $\text{CuS}$ ) in an inert atmosphere as a function of temperature [5].

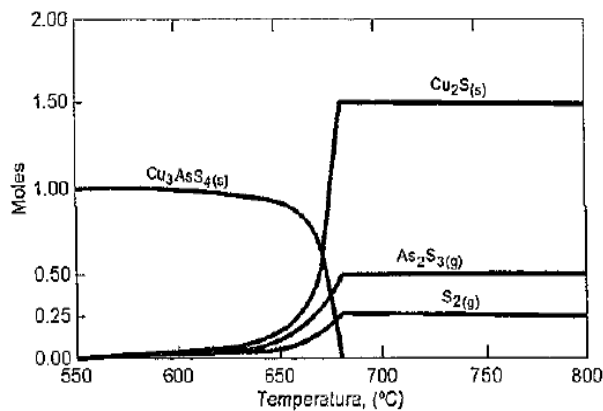


**Figure 3.** Equilibrium phases for the decomposition of enargite ( $\text{Cu}_3\text{AsS}_4$ ) in an inert atmosphere as a function of temperature [5].

From the above analysis [5], it was suggested that maximum arsenic volatilization occurs at  $700^\circ\text{C}$ .

Also, it was found that enargite ( $\text{Cu}_3\text{AsS}_4$ ) starts decomposing into copper sulfide ( $\text{Cu}_2\text{S}$ ) and arsenic trisulfide ( $\text{As}_2\text{S}_3$ ) at around  $650^\circ\text{C}$  and fully decomposed at  $670^\circ\text{C}$  (Figure 3) [5]. Similarly, covelite ( $\text{CuS}$ ) gets fully decomposed into copper (I) sulfide ( $\text{Cu}_2\text{S}$ ) and sulfur gas ( $\text{S}_2$ ) at  $600^\circ\text{C}$  (Figure 4). But pyrite ( $\text{FeS}_2$ ) needs higher temperature to form iron (II) sulfide ( $\text{FeS}$ ) and sulfur gas. It gets fully decomposed at slightly higher temperature of around  $700^\circ\text{C}$  (Figure 5).

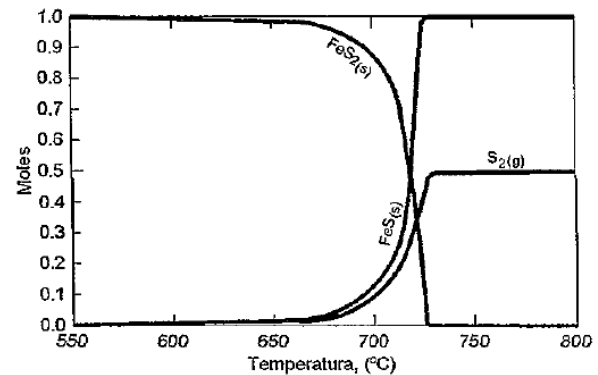


**Figure 5.** Equilibrium phases for the decomposition of pyrite ( $\text{FeS}_2$ ) in an inert atmosphere as a function of temperature [5].

Reaction mechanisms as discussed above, together with the thermodynamic data derived from pilot plant experiment, and analysis from thermochemical programming tool were integrated to build a model of the Fluidized Bed Roaster.

### Process Model

A process model consisting of fluidized bed roaster was built using IDEAS (Figure 6). Reactions (Table 1) along with the thermodynamic and kinetic data discussed in the previous section were used to model the Roaster. The steady state parameters used for the fluidized bed roaster (Table 4) was taken from pilot plant studies undertaken at the University of Concepcion, Chile.

The process model includes the roaster and the auxiliary units to completely collect formed calcine. Concentrate is fed from the top of the roaster. A start-up

burner preheats the initial sand bed of the roaster. The bed temperature is controlled by the water sprinklers. The existing gases are then passed through gas cyclones to collect the entrained calcine. Pressure inside the roaster is controlled by the speed of the intermediate fan after the gas cyclones. Calcine formed in the roaster is collected with the rotary feeders placed on the opposite side, at the bottom of the roaster. Speed of these feeders is controlled by the level of the fluidized bed formed in the roaster (Figure 6).

This dynamic process model was then used for the case study outlined in the following section.

### Case Study

A high arsenic percentage copper concentrate composition was considered for the experimental investigations. Table 2 shows the mineralogical composition of the concentrate used and Table 3 gives us the estimate of the elemental composition present.

**Table 2.** Mineralogical composition of concentrate feed.

	30
	22
	4.8
	7.3
	3.9
	26
	6

**Table 3.** Elemental composition of concentrate feed.

	42.76
	14.86
	32.2
	4.18
	6

**Table 4.** Steady state parameters used for the process model of fluidized bed roaster.

	75 tph*
	40,000 Nm <sup>3</sup> /h**
	250°C

Source: Pilot plant study at University of Concepcion, Chile (Unpublished work).

#Depends on air to concentrate ratio for desired extent of oxidation of sulfur [8].

\*tph corresponds to tonnes per hour.

\*\*Nm<sup>3</sup>/h corresponds to Normal cubic meter per hour.

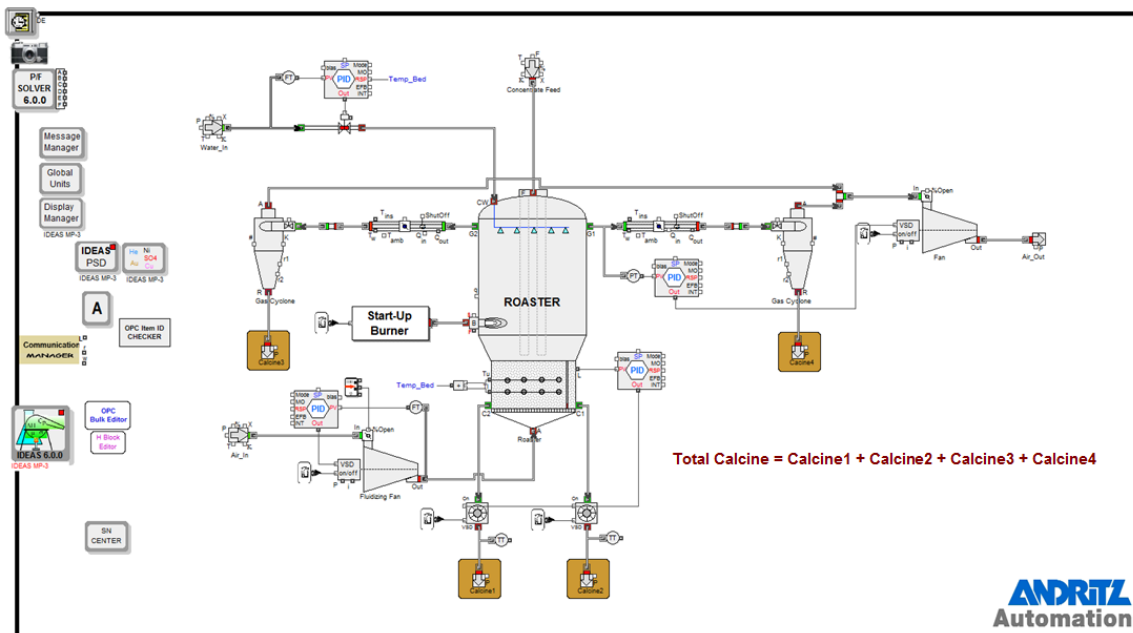


**Figure 6.** Overview of the process model of fluidized bed roaster built using IDEAS.

## Results and Discussion

Various simulation tests were performed with the dynamic process model built to simulate an actual plant. Behavior of the roaster was analyzed by varying process parameters such as feed rate, airflow rate, feed composition and cooling water rate.

It should be noted that the average temperature of the fluidized bed should be maintained at 700<sup>0</sup>C to possess maximum Arsenic volatilization (Figure 2).

As suggested, and later implemented by Wilkomirsky in the pilot plant, the following steps have to be followed to cold-start the roaster [1]:

1. Start the burner with zero airflow to preheat the sand bed in the roaster.
2. After the temperature of the bed reaches ~450<sup>0</sup>C, start the airflow to slowly stir the bed (~10,000 Nm<sup>3</sup>/h).
3. When the bed reaches its ignition temperature (~600<sup>0</sup>C), gradually increase the airflow and start the concentrate feeding.
  - 30 tph, ~20,000 Nm<sup>3</sup>/h fluidizing air with an estimated bed temperature of 625<sup>0</sup>C
  - 40 tph, ~25,000 Nm<sup>3</sup>/h fluidizing air with an estimated bed temperature of 650<sup>0</sup>C
4. Finally, end with the full concentrate feeding (75 tph) and airflow rate (~40,000 Nm<sup>3</sup>/h) to attain the steady state condition, the desired bed temperature of 700<sup>0</sup>C.

The following temperature profile (Figure 7) of the fluidized bed and off-gas from the roaster was generated and plotted to analyze the dynamic behavior while attaining the steady state condition.

In the plot (Figure 7), the fluidized bed gets stabilized at around 700<sup>0</sup>C with the use of cooling water. There is a temperature gap of around 25<sup>0</sup>C between the average fluidized bed temperature and the temperature of the off-gas from the roaster.

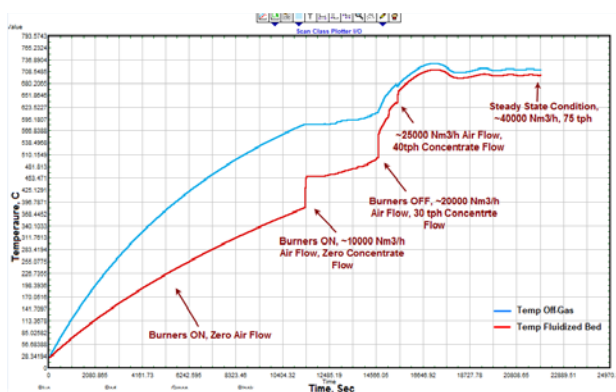


**Figure 7.** Steady state condition with 75 tph concentrate flow and 40,000 Nm<sup>3</sup>/h airflow rate as a function of time and temperature.

Four typical industrial scenarios were performed with the IDEAS process model.

### Effect Due to Change in the Concentrate Flow Rate

By following the cold start-up procedure mentioned, first the roaster was stabilized at 700<sup>0</sup>C with concentrate feed rate of 75 tph and airflow rate of 40,000 Nm<sup>3</sup>/h. Then, the following three cases were analyzed.

*Case 1:* Feed flow rate was increased to 90 tph with the same airflow rate of 40,000 Nm<sup>3</sup>/h.

*Case 2:* Feed flow rate was decreased to 65 tph with the same airflow rate of 40,000 Nm<sup>3</sup>/h.

*Case 3:* Feed flow rate was further decreased to 55 tph with the same airflow rate of 40,000 Nm<sup>3</sup>/h.

When the concentrate flow rate was increased to 90 tph, it was noted that the temperature of the bed started decreasing (Figure 8). This was mainly due to the non-availability of enough oxygen to oxidize the sulfur present, which is the main heat-generating reaction (Table 1). To overcome this, more airflow to the roaster is needed.

But, when the flow rate of the concentrate was decreased to 65 tph, the temperature of the bed increased considerably and increased further with decrease in the feed flow to 55 tph.

This study illustrates to a plant operator the effect of feed flow rate on process temperature while airflow is kept constant.

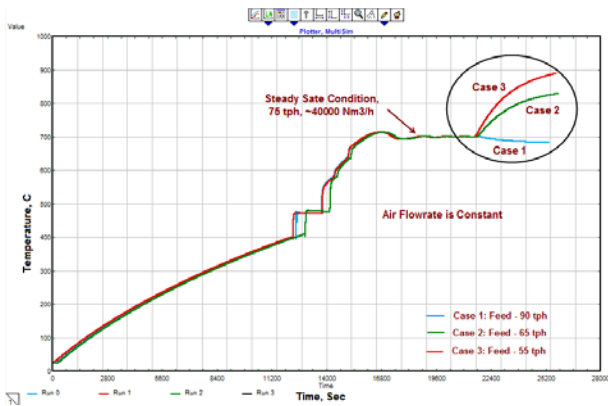


**Figure 8.** Behavior of the roaster on varying concentrate flow rate as a function of time and temperature.

**Effect Due to Change in the Fluidized Airflow Rate**

The fluidized airflow rate was varied to the roaster and its effect on the temperature profile of the fluidized bed and off-gas was analyzed. In this case also, first the roaster was stabilized at steady state. The following three cases are shown below:

*Case 1:* Fluidized airflow rate was increased to 55,000 Nm<sup>3</sup>/h with the same concentrate flow rate of 75 tph.

*Case 2:* Fluidized airflow rate was decreased to 45,000 Nm<sup>3</sup>/h with the same concentrate flow rate of 75 tph.

*Case 3:* Fluidized airflow rate was further decreased to 35,000 Nm<sup>3</sup>/h with the same concentrate flow rate of 75 tph.

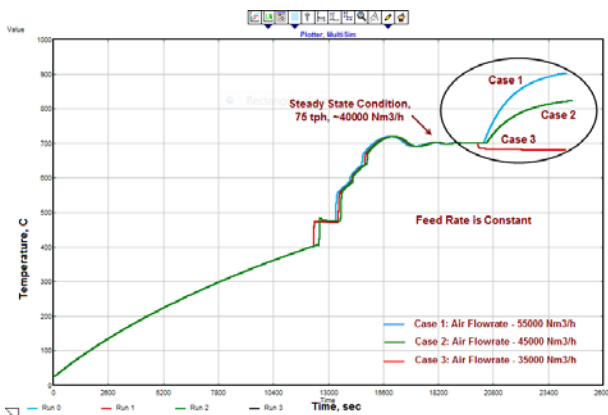


**Figure 9.** Behavior of the roaster on varying fluidizing airflow rate as a function of time and temperature.

As the flow rate of fluidized air was increased to 55000 Nm<sup>3</sup>/h, temperature of the fluidized bed increased to around 900°C (Figure 9). As more oxygen was passed through the bed, more sulfur was oxidized (Table 1).

When, the flow of air was decreased to 35,000 Nm<sup>3</sup>/h, the temperature of the bed started declining.

With the change in the fluidized airflow rate, arsenic volatilization (wt. % of arsenic going to off-gas) was also analyzed with all the three cases and plotted as shown in Figure 10. It can be noted that as we reduced the flow of air, arsenic wt. % going to the off-gas increased or there was less arsenic trapped in the calcine formed (Reaction 14 and 18).

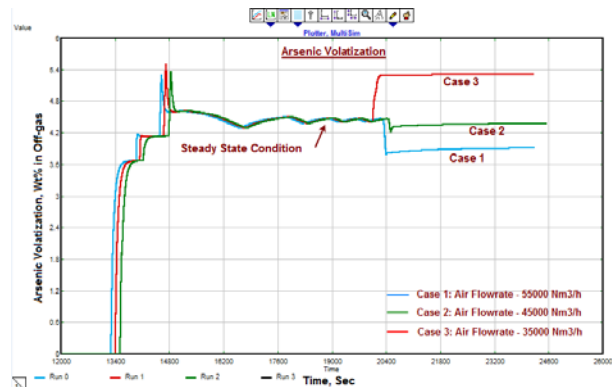


**Figure 10.** Behavior of the roaster and effect on arsenic volatilization on varying the airflow rate as a function of time.

The above study is essential for the plant operator to understand the effect of airflow rate on temperature profile and arsenic volatilization, while feed rate is kept constant.

**Effect Due to Change in the Bed Temperature and Cooling Water Rate**

Bed temperature in the roaster was varied and its effect on the rate of cooling water was analyzed. The following four cases are shown in Figure 11.

*Case 1:* Set point of the fluidized bed was at 700°C.

*Case 2:* Set point of the fluidized bed was increased to 720°C.

*Case 3:* Set point of the fluidized bed was further increased to 740°C.

*Case 4:* Set point of the fluidized bed was decreased to 680°C.

It can be seen that when the temperature of the fluidized bed was at 700°C, at steady state condition, cooling water rate was around 1900-2100 Litres/hour, but when the bed temperature was increased to 720°C, cooling water rate decreased subsequently (Figure 11). If we further increased the bed temperature, the cooling water rate also decreased. In case 4, when the bed temperature was decreased to 680°C, the cooling water rate increased accordingly.

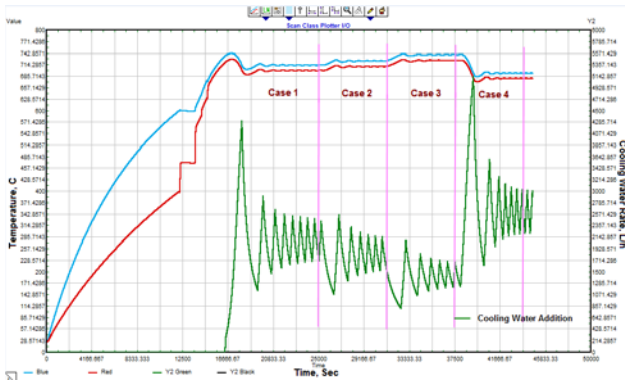


**Figure 11.** Behavior of the roaster on varying the bed temperature and effect on cooling water rate as a function of time.

This study illustrates the effect of cooling water rate on the temperature profile of the fluidized bed.

#### Effect Due to Change in the Feed Composition

Feed composition of the concentrate fed to the roaster was changed and its effects on the temperature profile of the fluidized bed were analyzed and compared with the below plot (Figure 12). Basically, arsenic percentage in the feed had changed.

A similar graph was plotted for the three cases and the same procedure was followed to cold-start the roaster as mentioned above to maintain a steady state condition at 700°C with the concentrate flow of 75 tph and fluidizing air at 40,000 Nm<sup>3</sup>/h.

Table 5 shows the mineralogical feed composition of the three cases used. Also, the elemental composition is shown in Table 6.

**Table 5.** Mineralogical composition of the concentrate feed for the cases used.

	30	25	34
	22	35	15
	4.8	4.8	4.8
	7.3	7.3	7.3
	3.9	3.9	3.9
	26	18	29
	6	6	6

**Table 6.** Elemental composition of the concentrate feed for the cases used.

Element	Case 1 (Wt/%)	Case 2 (Wt/%)	Case 3 (Wt/%)
Cu	42.76	45	42.57
Fe	14.86	11.13	16.25
S	32.2	31.14	32.2
As	4.18	6.65	2.85
Other	6	6.08	6.13

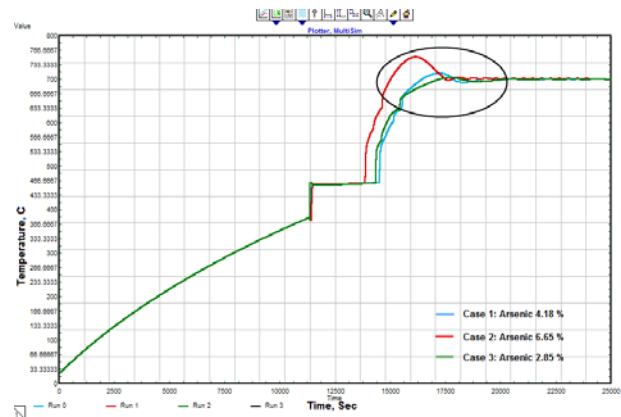


**Figure 12.** Behavior of the roaster on varying feed composition as a function of time and temperature.

From the marked area, it can be seen that the more the arsenic content concentrate (as in case 2), the more heat that was generated compared to the low arsenic content concentrate (Figure 13) in case 3.

This was because of the difference in the heat generated due to decomposition of enargite (Cu<sub>3</sub>AsS<sub>4</sub>) and pyrite (FeS<sub>2</sub>). Enargite decomposition generates more heat than that of pyrite (Table 1).



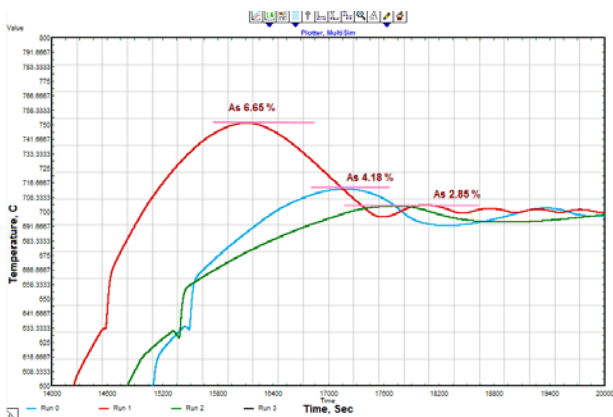


**Figure 13.** Behavior of the roaster on varying feed composition as a function of time and temperature (zoom in).

Also, a comparison was made on the behavior of fluidized bed roaster with respect to the arsenic volatilization going through the off-gas—between the concentrate having arsenic percentage of 6.65 (Figure 14) and that of 2.85 (Figure 15).

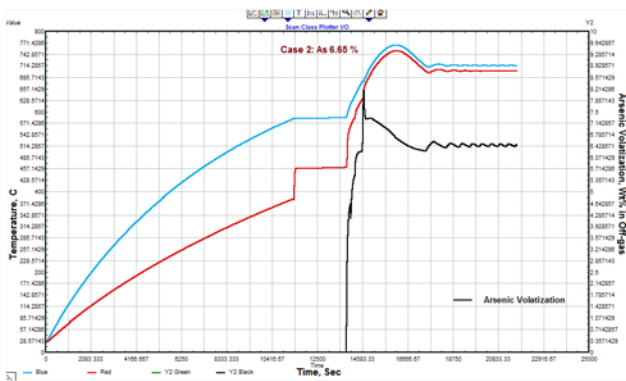


**Figure 14.** Behavior of the roaster having high arsenic content concentrate (6.65%) and the effect on arsenic volatilization while attaining steady state condition at 75 tph and 40,000 Nm<sup>3</sup>/h airflow rate.

As can be seen, more arsenic was volatilized to the off-gas in case 2 (As % 6.65) than in case 3 (As % 2.85).

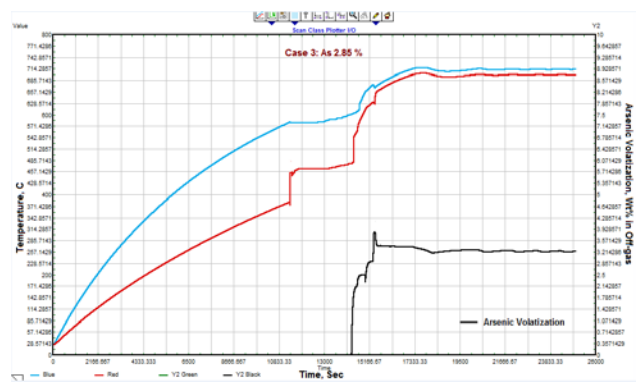


**Figure 15.** Behavior of the roaster having low arsenic content concentrate (2.85%) and effect on arsenic volatilization while attaining steady state condition at 75 tph and 40,000 Nm<sup>3</sup>/h airflow rate.

This study provides understanding of the effect of arsenic percentage on the temperature profile of the bed to the plant operators.

## Industrial Applications

The process model built using IDEAS has various industrial applications [14]. It can be used for:

- Validating Operating Procedures
- Testing What-If Scenarios
- Control Logic Verification
- Operator Training

*Validating Operating Procedures:* The virtual plant environment created can be of great help to understand and validate the operating procedures for start-up as well as shutdown. This can also be very useful to diagnose emergency faults in real time.

In the above case of the fluidized bed roaster, the cold-start operating procedure was validated with the use of IDEAS.

*Testing What-If Scenarios:* The process model can be useful to test the behavior of a particular unit operation under certain conditions, and subsequently, its effect on the operating parameters.

In the above study, four typical industrial scenarios were tested (Change in concentrate feed flow rate, airflow rate, cooling water rate, and concentrate feed composition), and their effects were shown on the temperature profile of the fluidized bed and arsenic volatilization.

*Control Logic Verification:* The process model can communicate with the control system, i.e., either Distributed Control System (DCS) and/or Programmable Logic Controller (PLC), and hence can be used for logic and control loop verification.

*Operator Training:* As the process model is connected to the actual plant control system, it can be used for operator training. The operators, with the use of real control screens, (or Human Machine Interface - HMI) can not only operate the plant but can also be trained to understand the process and equipment interactions.

## References

- [1] Boderill, J. S. M., Salway, A. G. and Teoman Y. (1983), "Heat conduction through slumped fluidized beds" at 4<sup>th</sup> Int. Conference on Fluidization, D. Kunii and R. Toei Eds., 315-330.
- [2] Chakraborti, N., and Lynch, D. C. (1983), "Thermodynamics of Roasting Arsenopyrite", in *Metallurgical Transactions*, 14B, 239-251.
- [3] Devia, M., Wilkomirsky, I. and Parra, R. (2012), "Roasting Kinetics of High-Arsenic Copper Concentrates: A Review", in *Minerals and Metallurgical Processing*, 121-128.
- [4] Downey, J. P., Eccleston, E. C. and Hager, J. P. (1999), "Application of Thermal Technology to Arsenic Remediation Problems", at San Sebastian, Spain: Rewas'99, *Global Symposium on Recycling, Waste Treatment and Clean Technology*, 1675-1683.
- [5] Fan, Y. (1997), "Cinetica y Mecanismos de Vaporizacion de Sulfuros de Arsenico desde Concentrados de Cobre", in *Tesis de Magister en Ciencias de la Ingenieria*, Mencion Metalurgia Extractiva, University of Concepcion, Concepcion, Chile.
- [6] Ferron, C. J. and De Cuyper, J. (1992), "The Recovery of Copper and Zinc from a Sulphide Concentrate using Sulphate Roasting, Acid Leaching and Solution Purification", in *International Journal of Mineral Processing*, 35, 225-238.
- [7] Holmstrom, A. (1989), "Removal of Arsenic from Gold-rich Concentrates by Roasting", in *Scandinavian Journal of Metallurgy*, 18, 12-30.
- [8] King, M. J., Sole, K. C. and Davenport W. G. I. (2011), in *Extractive Metallurgy of Copper*, Elsevier, 2011.
- [9] Lukanov, V. A., Shabalin, V. I. and Vasilevskiyi, O. V. (1982), "Autogenous Pyrrhotite Roasting of Pyrite Concentrate", in *Journal of Chemistry and Technology of Chalcogens and Chalcogenides*, 65, 249-251.
- [10] McCabe, J. A. and Morgan, C. L. (1956), "A Mechanism of Sulphate Formation During the Roasting of Cuprous Sulphide", in *Journal of Metals*, 8, 800A.
- [11] Padilla, R., Fan, Y., Sanchez, M. and Wilkomirsky, I. (1997), "Arsenic Volatilization from Enargite Concentrates", at *EPD Congress'97*, Concepcion, Chile.
- [12] Padilla, R., Fan, Y. and Wilkomirsky, I. (1999), "Thermal Decomposition of Enargite", at *EPD Congress'99*, 341-351.
- [13] Padilla, R., Fan, Y. and Wilkomirsky, I. (2001), "Decomposition of Enargite in Nitrogen Atmosphere", in *Canadian Metallurgical Quarterly*, Vol. 40, No. 3, 335-342.
- [14] Parthasarathi, P., Szaruga, V. and Szatkowski, M. (2009), "Benefits of Dynamic Simulation for Mineral Industry", in *Recent Advances in Mineral Processing Plant Design*, 84-92.
- [15] Peretti, E. A. (1948), "A New Method for Studying the Mechanism of Roasting Reactions", at *Discussions of the Faraday Society*, 4, 174-179.
- [16] Runkel, M. and Sturm, P. (2009), "Pyrite Roasting, an alternative to Sulphur Burning", in *The Journal of The Southern African Institute of Mining and Metallurgy*, 109, 491-496.
- [17] Secco, A. C., Riveros, G. A. and Luraschi, A. A. (1987), "Thermal Decomposition of Enargite and Phase Relations in the System Cu-As-S", at *Copper'87*, 225-238, Vina del Mar, Chile.
- [18] Smith, E. H. (1986), "Metallurgy and Mineral Processing at St. Joe's El Indio Mine in Chile", in *Mining Engineering*, 38, 971-979.
- [19] Wilkomirsky, I., Parra, R., Parra, F. and Balladares, E. (2013), "Physico-chemistry and Kinetics Mechanisms of Partial Roasting of High - Arsenic Copper Concentrates", at *Copper 2013*, Santiago, Chile.
- [20] Yoshimura, Z. (1962), "The Fundamental Investigation of De-arsenising Roasting of Copper Concentrates and its Industrial Practices", in *Journal of MMIJ*, 78, 447-453.
- [21] <http://gtt.mch.rwth-aachen.de/gtt-web/chemapp>.
- [22] <http://www.andritz.com/automation>